

Automatic conjunctival provocation test combining Hough circle transform and self-calibrated color measurements

Suman Raj Bista^{ab}, István Sárándi^a, Serkan Dogan^c, Anatoli Astvatsatourov^c, Ralph Mösges^c,
Thomas M. Deserno^a

^aDepartment of Medical Informatics, RWTH Aachen University, Aachen, Germany

^bUniversity of Burgundy, Le Creusot, France

^cDepartment of Medical Statistics, Informatics and Epidemiology,
University of Cologne, Cologne, Germany

ABSTRACT

Computer-aided diagnosis is developed for assessment of allergic rhinitis/rhinoconjunctivitis measuring the relative redness of sclera under application of allergen solution. Images of the patient's eye are taken using a commercial digital camera. The iris is robustly localized using a gradient-based Hough circle transform. From the center of the pupil, the region of interest within the sclera is extracted using geometric anatomy-based a-priori information. The red color pixels are extracted thresholding in the hue, saturation and value color space. Then, redness is measured by taking mean of saturation projected into zero hue. Evaluation is performed with 98 images taken from 14 subjects, 8 responders and 6 non-responders, which were classified according to an experienced otorhinolaryngologist. Provocation is performed with 100, 1,000 and 10,000 AU/ml allergenic solution and normalized to control images without provocation. The evaluation yields relative redness of 1.01, 1.05, 1.30 and 0.95, 1.00, 0.96 for responders and non-responders, respectively. Variations in redness measurements were analyzed according to alteration of parameters of the image processing chain proving stability and robustness of our approach. The results indicate that the method improves visual inspection and may be suitable as reliable surrogate endpoint in controlled clinical trials.

Keywords: Conjunctival Provocation Test (CPT), Allergic Rhinitis, Color Analysis, Hough Transform, Computer-Assisted Diagnosis (CAD), Surrogate Endpoint, Image-Based Endpoint

1. INTRODUCTION

Atopy (atopic syndrome) is pertaining to a hereditary tendency to experience immediate allergic reactions such as asthma or vasomotor rhinitis because of the presence of an antibody (atopic reagent) in the skin or the bloodstream. Worldwide, atopic diseases such as allergic rhinitis/rhinoconjunctivitis, allergic asthma and food allergy have increased.¹ This has been attributed to environmental factors, modulating genetic predisposition and the natural course of underlying allergic immune responses.² Preventive measures and immuno-modulatory treatment play an important role in the management of allergic diseases. Therefore, after establishing a tolerated dose range, a dose-response relationship for clinical efficacy must be established. Provocation tests (e.g. conjunctival, nasal or bronchial provocation or allergen exposure in allergen challenge chambers) and/or clinical endpoints may be used as primary endpoints in controlled clinical trials.

The conjunctival provocation test (CPT) has been introduced recently to document the course of allergic diseases and the effects of disease modifying treatments.³ It is a human model of ocular allergy that has been used to study the ocular response to allergenic stimuli and to evaluate antiallergic therapy.⁴ Usually, CPT is performed with grass pollen solutions of three different strengths. The redness of conjunctiva and sclera is assessed by visual inspection of an experienced physician or otorhinolaryngologist. However, qualitative inspection is highly observer-specific and too subjective as it could be used as a primary endpoint in a controlled clinical trial.⁵

Corresponding author: Thomas M. Deserno, Institut für Medizinische Informatik, Universitätsklinikum der RWTH Aachen, Pauwelsstr. 30, 52057 Aachen, Germany, Fon: +49 241 8088793, Fax: +49 241 803388792, Mail: deserno@ieee.org.

Medical Imaging 2013: Computer-Aided Diagnosis, edited by Carol L. Novak, Stephen Aylward, Proc. of SPIE
Vol. 8670, 86702J · © 2013 SPIE · CCC code: 1605-7422/13/\$18 · doi: 10.1117/12.2007821

Table 1: Categorization of response to allergen in CPT

Stage	Criteria
0	no subjective or visible reaction
I	itching, reddening, foreign body sensation
II	Stage I + tearing, vasodilation of conjunctiva and bulbi
III	Stage II + vasodilation and erythema of conjunctiva tarsi, blepharospasm
IV	Stage III + chemosis, lid swelling

In this paper, we present a novel method based on automatic processing of color images that is fast, reproducible, accurate, and applicable – at least in principle – to any photographic imaging device including low-cost consumer products.

2. MATERIALS AND METHODS

2.1. CPT protocol

The CPT has been standardized into five consecutive steps.

1. *Preparation*: The subject is adapted to the room climate for 10 minutes. Test solutions (expiry date, control temperature, body temperature required) are checked and it is confirmed that the eye is not irritated. Contraindications for CPT (eye diseases except for anomalies of refraction or allergic conjunctivitis, contact lenses, anti-allergic therapy) are excluded. The subject is informed to avoid rubbing his/her eyes during the entire procedure.
2. *Control*: 50 μl of control solution identical to the allergen solution except for allergen content is administered into the lower conjunctival sac of one eye (control eye).
3. *Provocation*: Immediately after application of control solution, 50 μl of low-concentrated allergen solution (100 AU/ml) is administered in the lower conjunctival sac of the opposite eye (provocation eye). 10 minutes wait time is taken.
4. *Evaluation*: The CPT is considered positive if the response is of Stage II or higher (Tab. 1).
 - If positive, topical antihistamine (e.g. levocabastine, azelastine, emedastine) is administered.
 - If negative, the provocation (Step 3) and evaluation (Step 4) loop is repeated with medium and – if again negative – with high concentrated solution of 1,000 AU/ml and 10,000 AU/ml, respectively.
5. *Termination*: The CPT is stopped.

2.2. Image recording

To derive quantitative measurements, a professional digital SLR (Olympus E3, Japan) with ring light (Hama LED Macro Light, DSLR, Germany) is used to record the eye of the patient. The macro light is composed of a ring with 12 LEDs for shadow-free illumination of subjects at color temperature of 5500 K. The camera is used in macro mode with automatic white adjustment disabled. Since the ambient light is dimmed during imaging, the illumination is defined by the LED source. Color calibration patterns are not yet applied, but can be integrated in the process easily.

The images are acquired after application of control solution or allergen solution. The image taken after administration of control solution (cf. Step 2 in Sect. 2.1) is taken as reference and measurement is done relative to this image. Figure 1 shows some examples: prominent variations in pupil positioning, focus and blur must be taken into account when designing robust segmentation.

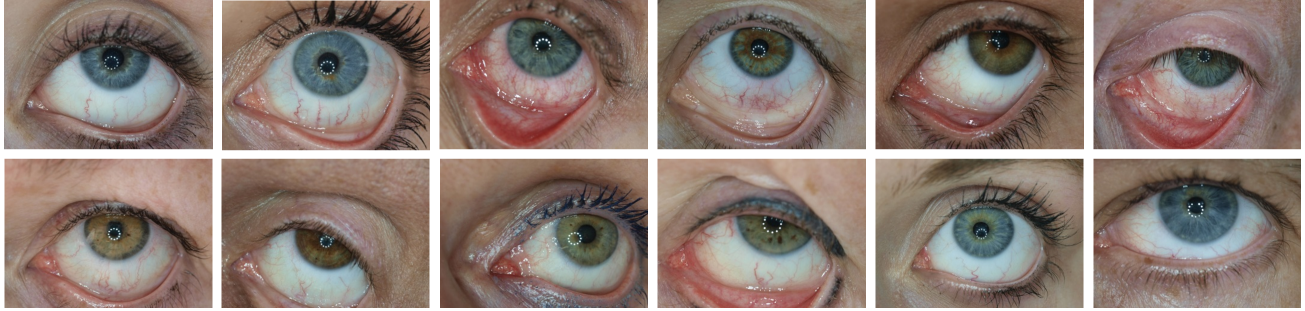


Figure 1: Images acquired for CPT

2.3. Image processing

The input to our system is the standardized image of the eye, showing the major portion of the sclera (Fig. 1). To segment the region of interest (ROI) of sclera, it is necessary to localize the eye in the image. The iris of the eye can be easily localized using its circular geometry. Based upon the center (x_c, y_c) and radius r of iris, the ROI is extracted using geometric anatomy-based a-priori information. The ROI images of a single patient are then aligned and masked to their intersection. This is needed in order to process the same region of the sclera in further steps. The red pixels of the segmented sclera are obtained by a thresholding operation in HSV space. Finally redness is measured by using hue and saturation information of the thresholded image. Figure 2 depicts the overall pipeline of the process.

2.3.1. Segmentation

Segmentation aims at the extraction of the sclera ROI. As emphasized in Fig. 1, the iris forms a prominently contrasted circle that is usable as a landmark. In order to localize the iris, the RGB image (Figs. 2a, 3a) is first converted to 8 bit grayscale format and the resolution is reduced from $3,648 \times 2,736$ pixels down to 256×192 pixels (Figs. 2b, 3b) using linear interpolation.⁶ The aspect ratio is conserved. Prominent edges are obtained using the Canny edge detection algorithm with the hysteresis approach, resulting in a binary image (Figs. 2c,

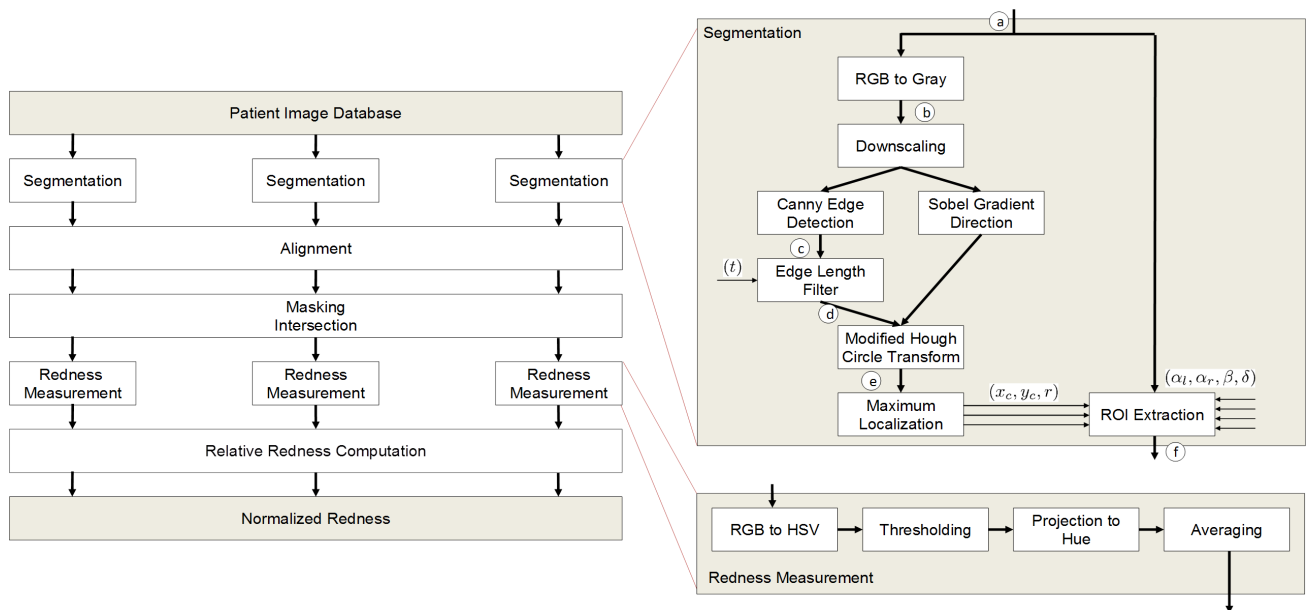


Figure 2: Image processing chain in overview (left) and segmentation as well as redness measurement chains in detail (right). The circled letters refer to Figure 3.

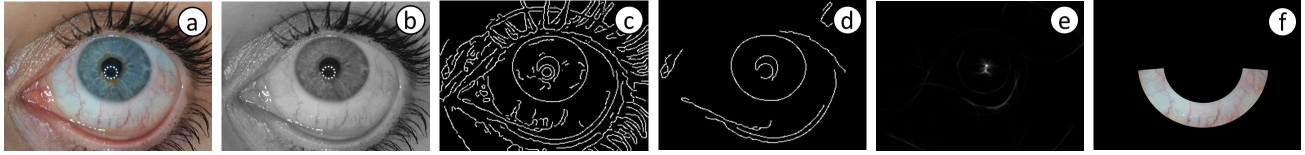


Figure 3: Intermediate step of the segmentation process. The letters refer to Figure 2.

3c). After applying connected components analysis, short segments are removed automatically (Figs. 2d, 3d). A minimum segment length of $t = 60$ pixels is applied. The purpose of this threshold is to ensure that the subsequent Hough circle transform detects the iris and not the boundary of the eyelids. Furthermore, image processing is speeded up. As an extension to the common Hough transform, the gradient direction is used to focus the maximum in Hough space and gain another boost in processing.⁷ In our implementation, the gradient is obtained by convolution with a Sobel kernel in horizontal and vertical orientation.

The iris circle is then detected using a directive circular Hough transform (Fig. 2e).^{7,8} Figure 3e illustrates the resulting three-dimensional (3D) accumulator array sliced at the radius r corresponding to the peak in Hough space. The peak is clearly indicated even if the iris is partly covered by the eyelid. After peak localization, the center and radius are projected back to original scale. The sclera region is then extracted from the original image (Figs. 2f, 3f).

Figure 4 illustrates how the sclera region is extracted using the circle of the iris obtained in the previous step. For this, a ring-shaped sector is used, extending from the center (x_c, y_c) of the iris. The two concentric circles have radius $(r + \delta)$ and $(\beta \cdot r)$, where δ and β denote according parameters. The two angles α_l and α_r for the left and right side, respectively, are used to extract a sector of the ring between the concentric circles.

The parameters δ , β , α_l and α_r have been individually determined for each image in the database in order to maximize the area of the ROI while containing only sclera parts. In detail, this shape is extracted as follows. First, a triangular mask (ΔOAB) is formed (Fig. 4). Since line segment \overline{AB} is tangent to the outer circle at N , the radius \overline{ON} is perpendicular to \overline{AB} at N . So, in right angle triangle ΔONA , side $\overline{AN} = \overline{ON} \cdot \tan \alpha_l = \beta \cdot r \cdot \tan \alpha_l$. Similarly, the right angle triangle ΔONB yields a side $\overline{BN} = \beta \cdot r \cdot \tan \alpha_r$. Hence, the coordinates of A and B can be easily calculated as $A = (x_c - \beta \cdot r \cdot \tan \alpha_l, y_c + \beta \cdot r)$ and $B = (x_c + \beta \cdot r \cdot \tan \alpha_r, y_c + \beta \cdot r)$, respectively. The ROI of the sclera is obtained as the intersection of the triangle ΔOAB and the outer circle of radius $\beta \cdot r$ minus the inner circle of radius $r + \delta$.

2.3.2. Alignment and intersection

In order to obtain a reliable sequence of redness values for a given patient, the same region of the sclera must be processed in each image of the patient (Fig. 2, left). To determine the relative redness, all images within a sequence must be registered. This process is illustrated in Fig. 5. Each image is translated and scaled such that the iris center and radius becomes the same for all images of the same patient. After this, the aligned sclera ROIs are intersected so that only the portion that is contained in all ROIs is kept for further processing (Fig. 5e,f).

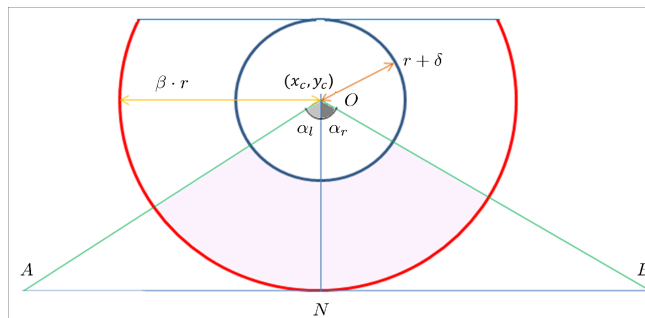


Figure 4: Extraction of the sclera ROI around the iris

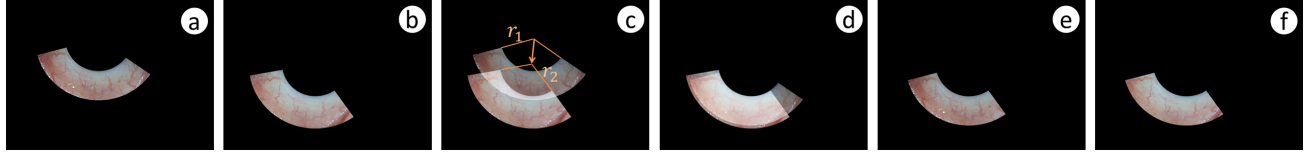


Figure 5: Illustration of alignment and intersection. Subimage (a) and (b) show the segmented sclera regions for two images of the same patient; (c) depicts their direct superimposition. After translation by the iris center difference and scaling by the ratio of the iris radii, the images become aligned (d). Finally, the resulting ROIs are intersected in (e), (f).

2.3.3. Redness measurement

The aim of redness measurement is to quantitatively determine the redness R of the sclera, since the blood vessels expand in response to the provocation, making the sclera redder.

The process of redness measurement is depicted in Fig. 2 (bottom right). First, the RGB image of the segmented sclera is converted into the Hue, Saturation, Value (HSV) color space (Fig. 6, left), which is better corresponding to semantic color concepts. Disregarding the value (indication of brightness), color is represented in the hue-saturation polar coordinate system. A symmetric section around the hue of H_0 with maximum deviation ΔH is extracted, where H_0 represents the mean red color of the vessels. All pixels that have a color outside of this hue range are discarded. In addition, all pixels with saturation lower than $S_0 = 0.01$ are also excluded from further evaluation (Fig. 6, right). The redness R is then measured by taking the mean of the saturation projected into zero hue

$$R = \frac{1}{n} \sum_{i=0}^{n-1} (S_i \cdot \cos H_i) \quad (1)$$

where n denotes the total number of red pixels after thresholding (Fig. 6, right).

The redness values obtained are not absolute because color calibration is not performed during image acquisition. However, our objective is to measure the relative change of redness after the application of different doses of allergen solution. To achieve this, the redness value before application of any allergen is taken as reference. The redness values obtained after application of control/allergen solution as described in CPT Protocol (cf. Step 2 in Sect. 2.1) are normalized with the value after the administration of the control solution without any allergen solution (Tab. 2).

2.4. Implementation

The overall system is developed in Java as an ImageJ plugin using Java Development Kit (JDK) version 1.6 update 33, ImageJ version 1.47a5 and NetBeans IDE 7.1.2. Some plugins from the ImageJ open source community are used with modification to suit our purpose. These are Canny Edge Detection,⁹ Connected Component Analysis,¹⁰ Hough Circles¹¹ and Color Space Transformation.¹² These plugins are modified such that automatic processing is enabled. This includes introducing constructors and methods to pass parameters and get results instead of using

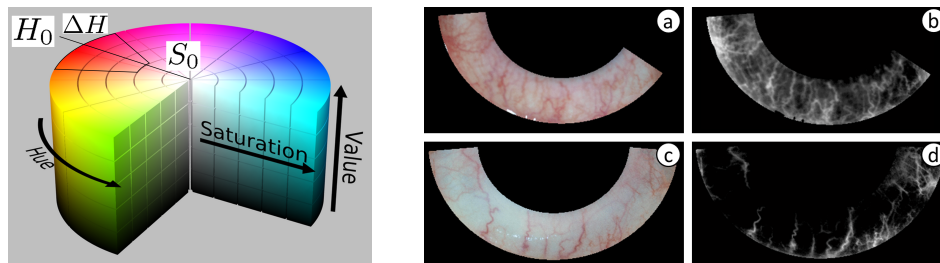


Figure 6: *Left*: Thresholding in HSV color space. *Right*: Sclera ROIs (a) and (b) and their corresponding red pixel thresholding for redness measurement (c) and (d), respectively.

Table 2: Relative redness measurements

Sequence	Dose	Redness value	Relative redness
0	0	R_0	1
1	100	R_1	$R_r^1 = R_1/R_0$
2	1,000	R_2	$R_r^2 = R_2/R_0$
3	10,000	R_3	$R_r^3 = R_3/R_0$

the graphical user interface (GUI), disabling GUI of these plugins when they are used from our Java program etc. Besides that, the Hough Circles plugin is modified to apply the gradient based Hough Circle Transform^{7,8} instead of the standard Hough Circle Transform⁸ present in original code.

2.5. Evaluation study

In a first evaluation study, 14 patients have been applied to 50 μ l of 100, 1,000, and 10,000 AU/ml concentrated allergen solution, consecutively. Visual inspection by an experienced otorhinolaryngologist categorizes the subjects into two groups, responders vs. non-responders, and 8 vs. 6 subjects resulted for each of the groups, respectively. Repeated measurements were made at each step of the CTP protocol (cf. Sect. 2.1). In total, 98 images have been acquired. Redness R for responders and non-responders were computed and normalized according to (1) and Table 2, yielding the relative redness R_r^i . Mean and standard deviation of R_r^i was determined.

Robustness was assessed varying the parameters (α_l, α_r) and t within a reasonable range. In particular, the intervals were set to $\alpha' = \alpha - p\alpha/100$ for $0 \leq p \leq 100$ and $0 \leq t \leq 100$, respectively. This is exemplified in Figure 7. Again, mean and standard deviation of R_r^i were monitored.

3. RESULTS

All photographs were processed successfully with our image processing chain. There were no drop outs due to variance in positioning or distortions. The Hough transform for iris localization performed errorless and accurate

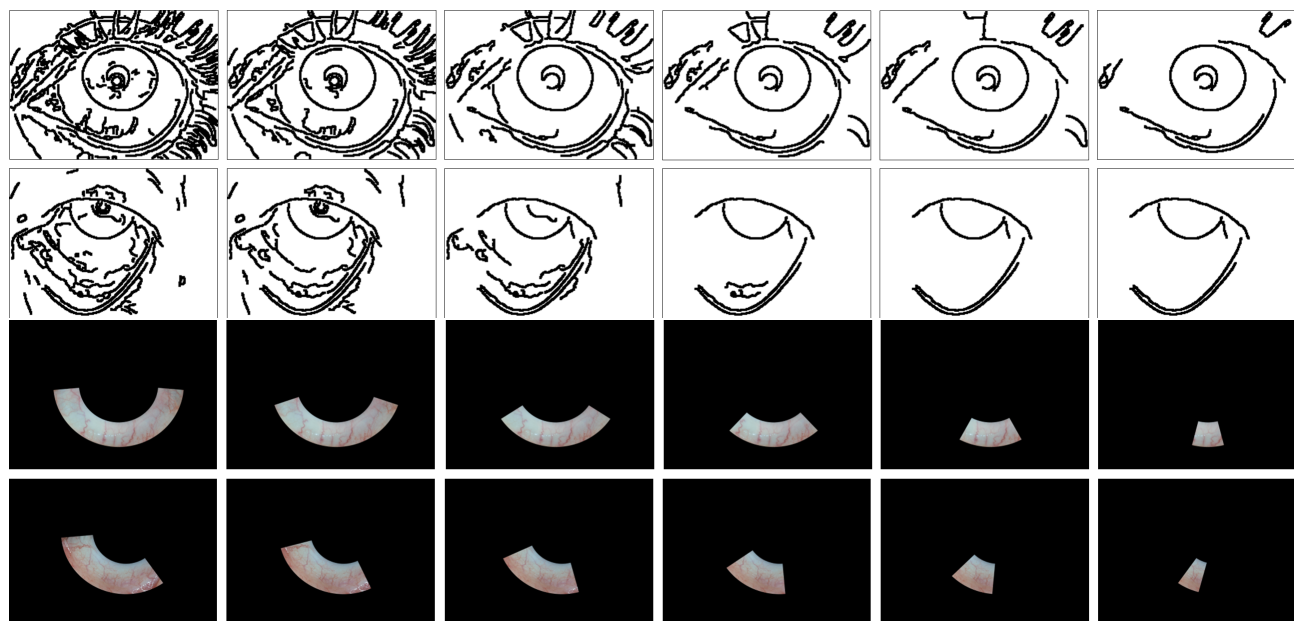


Figure 7: *Top*: Edge maps using different edge length thresholds ($t = 0, 20, 40, 60, 80, 100$). The image has been inverted and dilated for the illustration; *Bottom*: ROI extracted from the same image with successively shrinking α parameters.

Table 3: Results of responders

Patient Reference	Dose of Allergen Solution (AU/ml)	Repeated Measurements	Mean relative redness	Standard deviation
2009	0	1	1	–
	100	2	1.597	0.045
	1,000	2	1.383	0.042
	10,000	3	1.553	0.229
2010	0	1	1	–
	100	1	0.971	–
	1,000	3	0.917	0.019
	10,000	3	1.784	0.287
2012	0	1	1	–
	100	4	0.394	0.087
	1,000	2	0.381	0.038
	10,000	5	0.450	0.083
2013	0	1	1	–
	100	2	0.943	0.148
	1,000	2	1.044	0.318
	10,000	2	1.319	0.329
2014	0	2	1	0.039
	100	1	0.894	–
	1,000	1	1.035	–
	10,000	1	1.016	–
2016	0	1	1	–
	100	1	0.98	–
	1,000	2	0.938	0.025
	10,000	2	0.876	0.079
2117	0	1	1	–
	100	3	1.393	0.046
	1,000	2	1.958	0.139
	10,000	2	2.341	0.019
2118	0	1	1	–
	100	1	1.525	–
	1,000	2	0.764	0.088
	10,000	2	1.801	0.403
Mean	0	9	1	0.031
	100	15	1.014	0.449
	1,000	16	1.045	0.452
	10,000	20	1.297	0.656
Total no. of images		60		

for all images disregarding partial occlusion, blur, and noise. The detailed measurements are presented in Tables 3 and 4. While R_r^i is increasing with i for the responders, it is found to be rather constant for the non-responders.

In particular, for the group of responders, the relative redness is measured as 1.01, 1.05, and 1.30 for 100, 1,000 and 10,000 AU/ml, respectively. The group of non-responders yields 0.95, 1.00, and 0.96, respectively. Standard deviation for responders is significantly higher than for non-responders. Figure 8 summarizes the R_r^i -measures for both, responders and non-responders. The panels on the left and the right depict the same curves, but standard deviation is superimposed as box plot for responders and non-responders, respectively.

The outlier in Table 3 (Subject 2118) is due to incomplete opening of the eye, where the important part of

Table 4: Results of non-responders

Patient Reference	Dose of Allergen Solution (AU/ml)	Repeated Measurements	Mean relative redness	Standard deviation
2011	0	1	1	–
	100	1	1	–
	1,000	2	1.256	0.289
	10,000	2	1.285	0.018
2113	0	1	1	–
	100	2	1.016	0.029
	1,000	2	1.084	0.024
	10,000	2	0.936	0.001
2114	0	1	1	–
	100	1	1.227	–
	1,000	1	1.158	–
	10,000	2	0.963	0.066
2116	0	2	1	0.047
	100	1	0.809	–
	1,000	1	0.579	–
	10,000	2	0.931	0.033
2119	0	1	1	–
	100	2	0.756	0.038
	1,000	2	0.746	0.057
	10,000	2	0.798	0.007
2120	0	1	1	0
	100	1	1.014	0
	1,000	2	1.082	0.016
	10,000	3	0.87	0.187
Mean	0	7	1	0.039
	100	8	0.949	0.155
	1,000	10	1.007	0.258
	10,000	13	0.956	0.177
Total no. of images		38		

the sclera is covered by the lower eyelid. The corresponding photograph is depicted in Figure 1, lower right.

Figure 9 (left) shows the plot of mean relative redness for responded cases with respect to the edge threshold t that is used to alter the Canny edge detection step (Fig. 7, top). The redness measurements are almost constant. Figure 9 (right) shows the plot of mean relative redness for responded cases with respect to α . Although the redness values at different α depend upon the visibility of blood vessels (Fig. 7, bottom), alignment of regions again yields almost constant relative rednesses. Based on these results, the proposed method supports standardized CPTs and quantitative assessment of provocation response.

4. DISCUSSION AND CONCLUSION

A simple and robust image processing chain has been developed that quantifies conjunctival provocation test (CPT) making CPT applicable as primary end point in controlled clinical trials and for quantitative assessment of allergic diseases. The software correctly classifies responders and non-responders, which were verified by otorhinolaryngologist.

In this paper, we focused on frontal looking sclera for image processing and redness measurement. Off-angle sclera image segmentation and redness measurement is still challenging. So far, we do not apply color pattern and color calibration. This is likely to lower the standard deviation of the redness measure and enable also absolute color assessment. In Table 3, Subject 2012 results in R_r^i that drop to $R_r \approx 0.5$ for all provocation measures.

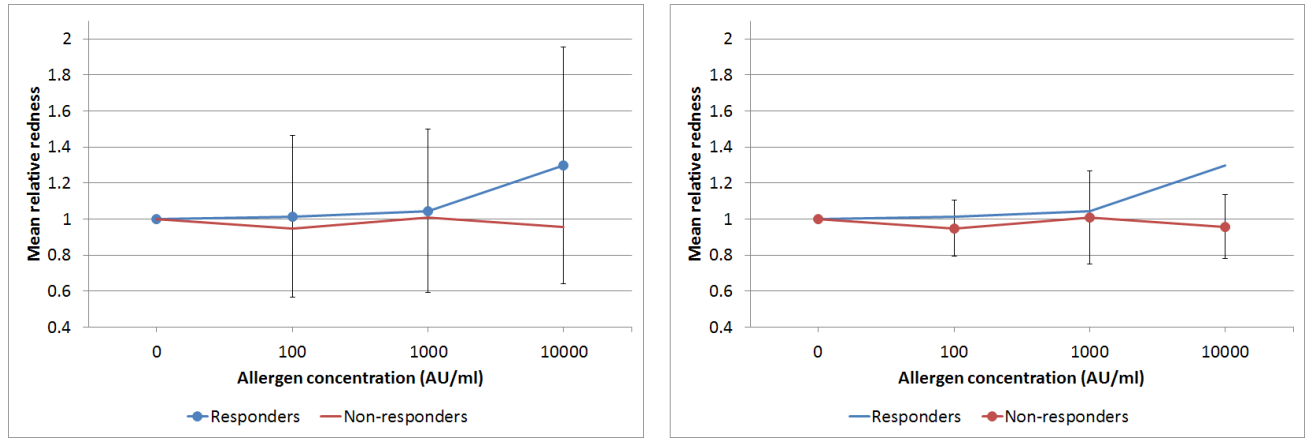


Figure 8: Plot of mean relative redness for responders and non-responders. The error bars on the left and right refer to standard deviation for responders and non-responders, respectively.

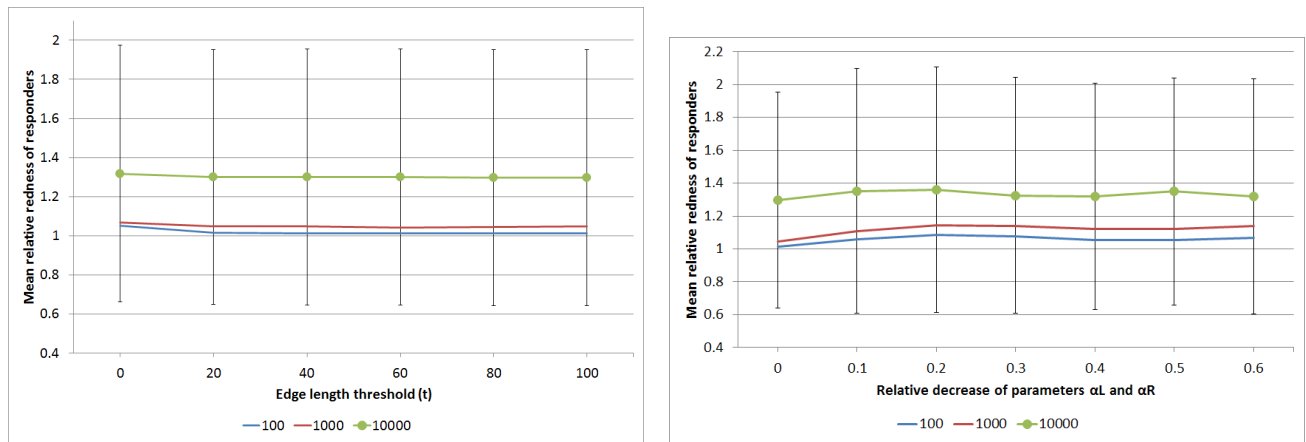


Figure 9: *Left*: Relative redness w.r.t. edge length threshold (t) for responded cases. The error bars represent the standard deviation for the 10,000 AU/ml dose measurements; *Right*: Mean relative redness w.r.t. α for responders. The error bars present the standard deviation for the 10,000 AU/ml dose measurement.

Figure 10 depicts some of the source images. As it can be clearly noticed, the direction of view was changed between the baseline R_0 and all follow-up images R_i , $i = \{1, 2, 3\}$. Since the eyeball is sphere-shaped, geometric distortions in projection result for the sclera ROI (Fig. 10, bottom row). Such distortions cannot be corrected with our translational registration. Hence, a more complex ROI adjustment might be helpful. Furthermore, the imaging protocol needs standardization regarding the optical axis of the eye. This might be done applying an fixation light-emitting diode (LED) and ask the subjects to focus the light during imaging.

In this study, a professional SLR camera was used, with automatic white adjustment disabled. For large parts of the automatic processing chain, image resolution was reduced to 256×192 pixels. Only color measurement was performed on the ROI extracted from the high-resolution images. Nonetheless, due to blurred and unfocused imaging, such a high resolution is not required, which will support a future system design using low-cost consumer cameras, which also are lighter in weight and easier in use.

Also, the parameters α , β , and δ will be determined automatically in future. This can be done adding some heuristics into the chain of image processing. Then, the entire process becomes fully automatic. However, our small evaluation study has already shown that the relative redness is increased significantly for the group of responders, whilst a rather constant redness is obtained for those subjects that have been rated as non-responder. In summary, we conclude that the proposed image processing chain improves visual inspection and is suitable for

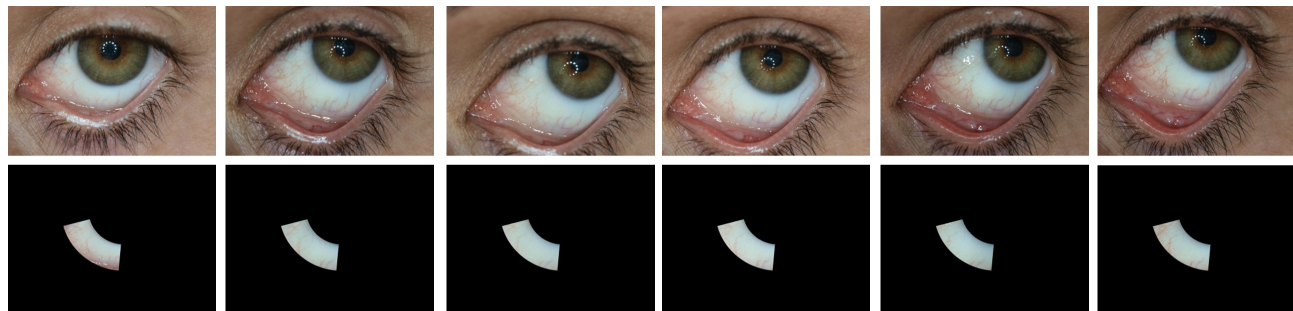


Figure 10: Images and ROIS for some images of Subject 2012. Form *left to right*: R_0 , R_1 , R_1 , R_2 , R_3 , R_3 ; *Top*: source images, *bottom*: sclera ROI. Note the different direction of view between baseline and all follow-up images.

computer-aided diagnosis in allergic rhinitis/rhinoconjunctivitis. In future, it may become a reliable surrogate endpoint in controlled clinical trials.

REFERENCES

1. Ait-Khaled N, Pearce N, Anderson H, et al. Global map of the prevalence of symptoms of rhinoconjunctivitis in children: the international study of asthma and allergies in childhood (ISAAC) phase three. *Allergy*. 2009;64(1):122–148.
2. Mösges R, Klimek L. Today's allergic rhinitis patients are different: new factors that may play a role. *Allergy*. 2007;62(9):969–975.
3. Riechelmann H, Epple B, Gropper G. Comparison of conjunctival and nasal provocation test in allergic rhinitis to house dust mite. *Int Arc Allergy Immunol*. 2003;130(1):51–59.
4. Friedlaender MH. Conjunctival provocation testing: overview of recent clinical trials in ocular allergy. *Curr Opin Allergy Clin Immunol*. 2002;2(5):413–7.
5. Jüni P, Altman DG, Egger M. Systematic reviews in health care: assessing the quality of controlled clinical trials. *Br Med J*. 2001;7(323(7303)):42–6.
6. Lehmann TM, Gonner C, Spitzer K. Addendum: B-spline interpolation in medical image processing. *IEEE Trans Med Imaging*. 2001;20(7):660–665.
7. Kaupp A, Lehmann T, Effert R, et al. Automatic measurement of the angle of squint by Hough-transformation and covariance-filtering. *Proc 12th Conf Int Ass Pattern Recogn (IAPR)*. 1994;1:784–6.
8. Ballard DH, Brown CM. *Computer Vision*. Englewood Cliffs, NJ: Prentice-Hall; 1982.
9. Meijering E. FeatureJ: A Java Package for Image Feature Extraction;. [Online; accessed on 04-09-2012]. <http://www.imagescience.org/meijering/software/featurej/>.
10. Longair M. Find Connected Regions;. [Online; accessed on 04-09-2012]. <http://www.longair.net/edinburgh/imagej/find-connected-regions/>.
11. Pistori H, Costa ER. Hough Circles;. [Online; accessed on 03-09-2012]. <http://rsbweb.nih.gov/ij/plugins/hough-circles.html>.
12. E Barilla M. Color Transformer;. [Online; accessed on 04-09-2012]. <http://rsbweb.nih.gov/ij/plugins/color-transforms.html>.